Clin Orthop Relat Res (2013) 471:834–842
DOI 10.1007/s11999-012-2560-8

Clinical Orthopaedics and Related Research®
A Publication of The Association of Bone and Joint Surgeons®

SYMPOSIUM: HIGHLIGHTS FROM THE FIRST COMBINED 2011 MEETING OF THE MUSCULOSKELETAL TUMOR SOCIETY AND CONNECTIVE TISSUE ONCOLOGY SOCIETY

A Novel Imaging System Permits Real-time in Vivo Tumor Bed Assessment After Resection of Naturally Occurring Sarcomas in Dogs

William C. Eward DVM, MD, Jeffrey K. Mito MD, PhD, Cindy A. Eward DVM, Jessica E. Carter, Jorge M. Ferrer PhD, David G. Kirsch MD, PhD, Brian E. Brigman MD, PhD

Published online: 13 September 2012

Abstract

Background Treatment of soft tissue sarcoma (STS) includes complete tumor excision. However, in some patients, residual sarcoma cells remain in the tumor bed. We previously described a novel hand-held imaging device prototype that uses molecular imaging to detect microscopic residual cancer in mice during surgery.

Questions/purposes To test this device in a clinical trial of dogs with naturally occurring sarcomas, we asked: (1) Are any adverse clinical or laboratory effects observed after intravenous administration of the fluorescent probes? (2) Do canine sarcomas exhibit fluorescence after administration of the cathepsin-activated probe? (3) Is the tumor-to-background ratio sufficient to distinguish tumor from tumor bed? And (4) can residual fluorescence be detected in the tumor bed during surgery and does this correlate with a positive margin?

Methods We studied nine dogs undergoing treatment for 10 STS or mast cell tumors. Dogs received an intravenous injection of VM249, a fluorescent probe that becomes optically active in the presence of cathepsin proteases. After injection, tumors were removed by wide resection. The tumor bed was imaged using the novel imaging device to search for residual fluorescence. We determined correlations between tissue fluorescence and histopathology, cathepsin protease expression, and development of recurrent disease. Minimum followup was 9 months (mean, 12 months; range, 9–15 months).

Results Fluorescence was apparent from all 10 tumors and ranged from 3×10^7 to 1×10^9 counts/millisecond/cm^2. During intraoperative imaging, normal skeletal muscle showed no residual fluorescence. Histopathologic assessment of surgical margins correlated with intraoperative imaging in nine of 10 cases; in the other case, there was no residual fluorescence, but tumor was found at the

The institution of one or more of the authors has received funding, during the study period, from an NIH CTSA grant (UL1RR024128) from the Duke Translational Research Institute (BEB), the Damon Runyon-Rachleff Innovation Award (DGK), and a Fitzgerald Scholarship (JEC). Two of the authors (DGK and JMF) certify that they have received or may receive payments or benefits, during the study period, an amount of $10,000 to $100,000, from Lumicell Diagnostics, Inc (Waltham, MA, USA), a company commercializing in vivo imaging systems. Two of the authors (DGK and JMF) certify that they are members of the scientific advisory board for Lumicell Diagnostics, Inc.
All ICMJE Conflict of Interest Forms for authors and *Clinical Orthopaedics and Related Research* editors and board members are on file with the publication and can be viewed on request.
Each author certifies that his or her institution approved the animal protocol for this investigation and that all investigations were conducted in conformity with ethical principles of research.
This work was performed at Duke University Medical Center (Durham, NC, USA) and the Veterinary Specialty Hospital of the Carolinas (Cary, NC, USA).

W. C. Eward (✉)
Department of Orthopaedic Surgery, Duke University Medical Center, Box 3312 DUMC, Durham, NC 277710, USA
e-mail: w.eward@alumni.duke.edu; william.eward@duke.edu

J. K. Mito
Department of Pharmacology & Cancer Biology, Duke University Medical Center, Durham, NC, USA

C. A. Eward
Veterinary Specialty Hospital of the Carolinas, Cary, NC, USA

J. M. Ferrer
Department of Chemistry, Massachusetts Institute of Technology, Cambridge, MA, USA

margin on histologic examination. No animals had recurrent disease at 9 to 15 months.
Conclusions These initial findings suggest this imaging system might be useful to intraoperatively detect residual tumor after wide resections.
Clinical Relevance The ability to assess the tumor bed intraoperatively for residual disease has the potential to improve local control.

Introduction

Current treatment for soft tissue sarcoma (STS) includes complete excision of the tumor with a surrounding margin of normal tissue such that no malignant cells remain in the tumor bed. The presence of residual sarcoma cells in the tumor bed is associated with local recurrence and decreased disease-specific survival [10, 15, 17, 18]. At present, surgical margin status is determined by the evaluation of the resected specimen by a pathologist. A comprehensive assessment of surgical margins requires days to weeks to complete and, for large STSs, is prone to sampling error [17]. For patients with tumor cells present at the margin of the resected specimen, additional therapy is required to achieve local control. This may include repeat surgical resection and/or adjuvant radiation therapy with its attendant increase in patient morbidity and healthcare costs.

These factors have led to great interest in approaches that allow surgical margin assessment at the time of the initial resection. Available approaches for intraoperative margin assessment using ultrasound [6], radiofrequency spectroscopy [1], and frozen sections [14] have limitations. Intraoperative ultrasound has little capacity for magnification and is not likely to detect small residual collections of tumor. Radiofrequency spectroscopy is technically complex and not readily adaptable to the live operative setting. Frozen sections are time consuming and are subject to sampling error, especially in the large tumor beds associated with sarcoma resection.

To address this unmet clinical need for real-time, intraoperative assessment of microscopic residual sarcoma in the tumor bed, we collaborated with engineers from Massachusetts Institute of Technology (Cambridge, MA, USA) to develop a novel, wide-field-of-view imaging system that, when coupled with a near-infrared (NIR) fluorescent probe, can resolve microscopic clusters of tumor cells [12]. The NIR probe becomes optically active when cleaved by cathepsin proteases. We have demonstrated, in a genetically engineered mouse model of STS [13], these NIR probes are selectively activated in sarcomas because cathepsin proteases are overexpressed in STSs in mice [8, 12]. We used the system in mice with genetically engineered STSs to detect residual NIR fluorescence within the tumor bed [12]. The mice underwent intralesional, marginal, and wide resection of their tumors. Intraoperative fluorescent imaging results were correlated with histopathology and the mice were followed clinically for local recurrence. The presence of residual fluorescence correlated with local recurrence, and resection of this residual NIR fluorescence improved local control. Despite the ability to image residual tumor in mice, it is unclear whether this technology can be successfully translated into the clinic where spontaneous tumors arise from a more diverse set of initiating gene mutations, which might affect cathepsin protease expression [2]. In addition, because the mouse sarcomas are relatively small (approximately 1–2 cm), results of surgical studies in mice may not fully translate to surgery in patients with large sarcomas (5–15 cm).

Sarcomas occur much more commonly in dogs, accounting for 15% of all tumors [5]. The primary therapy for canine STS, as in humans, is resection of the tumor with negative surgical margins [5]. Therefore, to test this imaging system in spontaneous tumors in a clinical setting, we initiated a canine clinical trial.

In this clinical trial in dogs with naturally occurring sarcomas, we answered the following questions: (1) Are any adverse clinical or laboratory effects observed after intravenous administration of the fluorescent probes to dogs undergoing resection of sarcomas? (2) Do naturally occurring canine sarcomas exhibit fluorescence after administration of the cathepsin-activated probes? (3) If so, is the tumor-to-background ratio sufficient to distinguish tumor from normal tumor bed during resection of naturally occurring canine tumors? And (4) can residual NIR fluorescence be detected in the tumor bed in the live operative setting and does this correlate with a positive margin of the resected tumor?

Materials and Methods

Between November 2010 and May 2011, we treated a total of 30 dogs for tumors identified by biopsy as either STS or

J. E. Carter, D. G. Kirsch
Department of Pharmacology & Cancer Biology,
Duke University Medical Center, Durham, NC, USA

J. E. Carter, D. G. Kirsch
Department of Radiation Oncology, Duke University
Medical Center, Durham, NC, USA

B. E. Brigman
Department of Orthopaedic Surgery,
Duke University Medical Center,
Durham, NC, USA

Table 1. Summary of subject data

Dog	Age (years)	Weight (kg)	Breed	Diagnosis	Residual tumor bed fluorescence†	Histopathologic margins	Recurrent disease
1	6.8	19.8	Brittany	MPNST	Negative	Negative	No
2	7	20	Australian cattle dog	UPS	Negative	Negative	No
3	9.9	30.1	Labrador	MPNST	Negative	Negative	No
4	6.6	34.3	Mixed breed	MCT	Positive	Positive	No
5	6	22.3	Bassett hound	MCT	Negative	Negative	No
6	9.3	39.1	Labrador	MPNST	Negative	Positive	No
7	5	37.6	Mixed breed	MCT	Negative	Negative	No
8	11	14.4	Bassett hound	MCT	Negative	Negative	No
9*	12	7.9	Schnauzer	Fibrosarcoma	Negative	Negative	No
9*	12	7.9	Schnauzer	MPNST	Negative	Negative	No

* Dog 9 had two different sarcomas; †visually detectable fluorescence was calibrated based on imaging of a cut surface of the resected tumor; an intensity threshold to image residual fluorescence was set based on 80% of the minimum fluorescence emission rate from each tumor; pixels from the tumor bed image with emission rates at or above the threshold were identified in real time using an automatic software routine; MPNST = malignant peripheral nerve sheath tumor; UPS = undifferentiated pleomorphic sarcoma; MCT = mast cell tumor.

canine mast cell tumor (MCT) (a malignancy of soft tissues, which is similar to STS). Each dog presented to the Veterinary Specialty Hospital of the Carolinas for treatment by a multidisciplinary small-animal oncology team. Five dogs had underlying organ dysfunction (four with chronic renal insufficiency, one with hepatic insufficiency) and their owners were not offered enrollment. We offered enrollment to the owners of the remaining 25 dogs, but 14 declined to participate, leaving 11 dogs (12 tumors) for potential participation in the study. Of the 12 tumors, two tumors (two dogs) were found not to have sarcomas based on final histopathology. One dog had a history of previous incomplete excision of a STS on the ventral chest wall. Repeat excision of the tumor bed revealed no residual tumor on gross or microscopic evaluation. One dog with a periumbilical mass believed to be STS based on core needle biopsy showed necrosis, fibrosis, and chronic inflammation but no identifiable neoplasia. These two dogs were excluded from analysis, leaving 10 tumors in nine dogs for analysis (Table 1). There were five males and four females. No single breed was represented more than twice. Mean age was 9.5 years (range, 5–12 years). Mean body weight was 25 kg (range, 7.9–39.1 kg). Minimum followup was 10 months (mean, 13 months; range, 9–16 months). No dog was lost during the period of followup. Histopathologic diagnoses included six STSs in five dogs and MCTs in four dogs. We had prior approval from the Duke University Institutional Animal Care and Use Committee (Duke IACUC Protocol A213-10-08).

As shown in the optical layout of the imaging device (Fig. 1A), the device employs white light illumination for excitation and a set of spectral filters (excitation filter, dichroic mirror, and emission filter) for fluorescence imaging. Several lenses are used to relay the fluorescence image at no magnification into a charge-coupled device where the fluorescence emission of individual cancer cells is mapped into 2 to 4 pixels. The device was essentially similar to that previously reported [12] but was subsequently modified in several important ways to facilitate its use in the operating room. First, the bench-mounted prototype was adapted for use on a rolling platform that could be brought to adjustable proximity and location relative to the operating table. Second, because the original surgeries in mice were semisterile, the device was adapted for sterile use. Sterilizable sleeves and a sterilizable objective lens cover were custom-made so that the device could be used in a fully sterile fashion. The computer display was adapted for use on a rolling platform so that it could be readily seen by the surgeon. Additionally, the display was modified so that fluorescence above the desired threshold would be displayed in red on the visual display to allow for rapid detection of residual fluorescence.

After obtaining informed consent from the owners, the dogs were given a dose of the cathepsin-activated NIR imaging probe VM249 (Visen Medical/Perkin Elmer, Waltham, MA, USA; dose range, 0.5–2 mg/kg) by intravenous injection. Dogs were kept in the intensive care unit after injection of the probe and for 24 hours after surgery to monitor for adverse effects, namely anaphylaxis, injection site inflammation, or behavioral changes. In all dogs, a baseline preoperative CBC and serum biochemistry profile had been obtained. In six dogs, a postoperative CBC and serum biochemistry profile were obtained on Postoperative Day 1. In five dogs, these tests were declined by the owners due to cost concerns. The first two dogs had surgery 6 hours after injection as this time point had worked in the

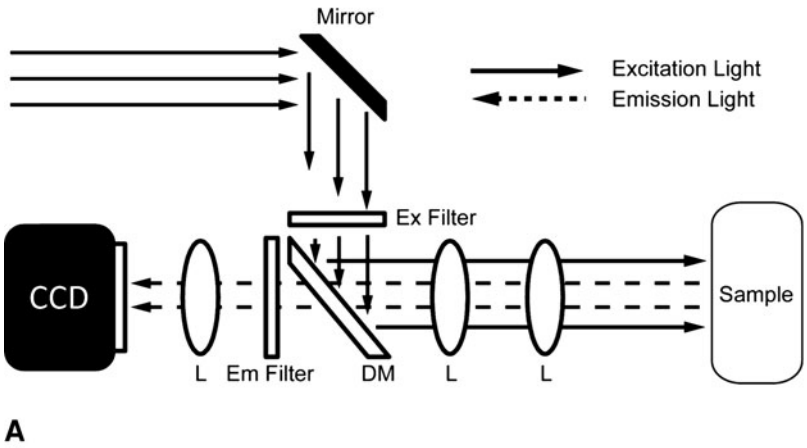

Fig. 1A–B (**A**) A diagram illustrates the optical layout of the intraoperative imaging device. Light enters the device through the fiber bundle where it is reflected through an excitation filter (ex filter) and reflected with a dichroic mirror (DM) onto the tumor sample/tumor bed where emitted light returns through the emission filter (em filter) to the detector. Several lenses (L) are used to relay the fluorescence image at no magnification into a charge-coupled device (CCD) where the fluorescence emission of individual cancer cells is mapped into 2 to 4 pixels. (**B**) A photograph shows the device in use in a dog with a chest wall STS.

mouse studies [12]. To account for potential differences in pharmacokinetic parameters between mice and dogs, the remaining dogs were imaged at 24 hours after injection. Standard wide or radical resection of the tumor was performed by a board-certified veterinary surgeon (CAE). The resected specimen was removed from the operative field and incised to expose the tumor. The exposed portion of the tumor was imaged with the device and pixel intensity values were normalized by exposure time to obtain a time-independent fluorescence emission rate. Based on our previous experience in mice [12], an intensity threshold to image residual NIR fluorescence was set based on 80% of the minimum fluorescence emission rate from each tumor. Resected tumors were then inked and transported to the histopathology laboratory.

After setting the threshold, the imaging device was covered with a sterile sleeve and brought into the operative field. The operating surgeon used the device to scan the entire tumor bed (specifically all exposed tissue) (Fig. 1B). Because this technology is investigational, we did not have approval to modify the operative plan (ie, resect more tissue) based on imaging results. The time required to image the tumor and the tumor bed was approximately 15 minutes/tumor. Pixels from the tumor bed image with emission rates at or above the threshold were identified in real time using an automatic software routine [12]. After surgery, three of us (JKM, JEC, JMF) also analyzed images obtained at the time of surgery to ensure correct intraoperative assessment. The tumor bed was classified as having either positive or negative residual fluorescence based on the threshold calibration. The wound was irrigated and closed. Postoperative care was routine and was not affected by enrollment in this study. Biopsies of the resected tumor and tumor bed were submitted to two different veterinary pathologists for histopathologic analysis and comparison with imaging results.

To determine whether positive fluorescence correlated with the presence of cathepsin proteases within tumors (and the absence of cathepsin proteases within surrounding muscle), muscle-normalized transcription of RNA for cathepsins B, K, L, and S (each of which cleave VM249) was quantitatively measured via real-time PCR using the iTaq™ SYBR® Green supermix (Bio-rad Laboratories, Inc, Hercules, CA, USA) with the following primers: cathepsin B: 5′-TGCGGTTCCTGCTGGGCATTT-3′ and 5′-TGACGTGCCCATTGGTGCGG-3′; cathepsin L: 5-TTGGAAGGGACACAGAGACCTGCA-3′ and 5′-GGGCCTTCTCCCGTTGAGGGAG-3′; cathepsin K: 5′-ACCAGGGTCAGTGTGGTTCCTGTT-3′ and 5′-GATGGGTCCCACTCGGGCCA-3′; and cathepsin S: 5′-TTGGGCTGCTTC

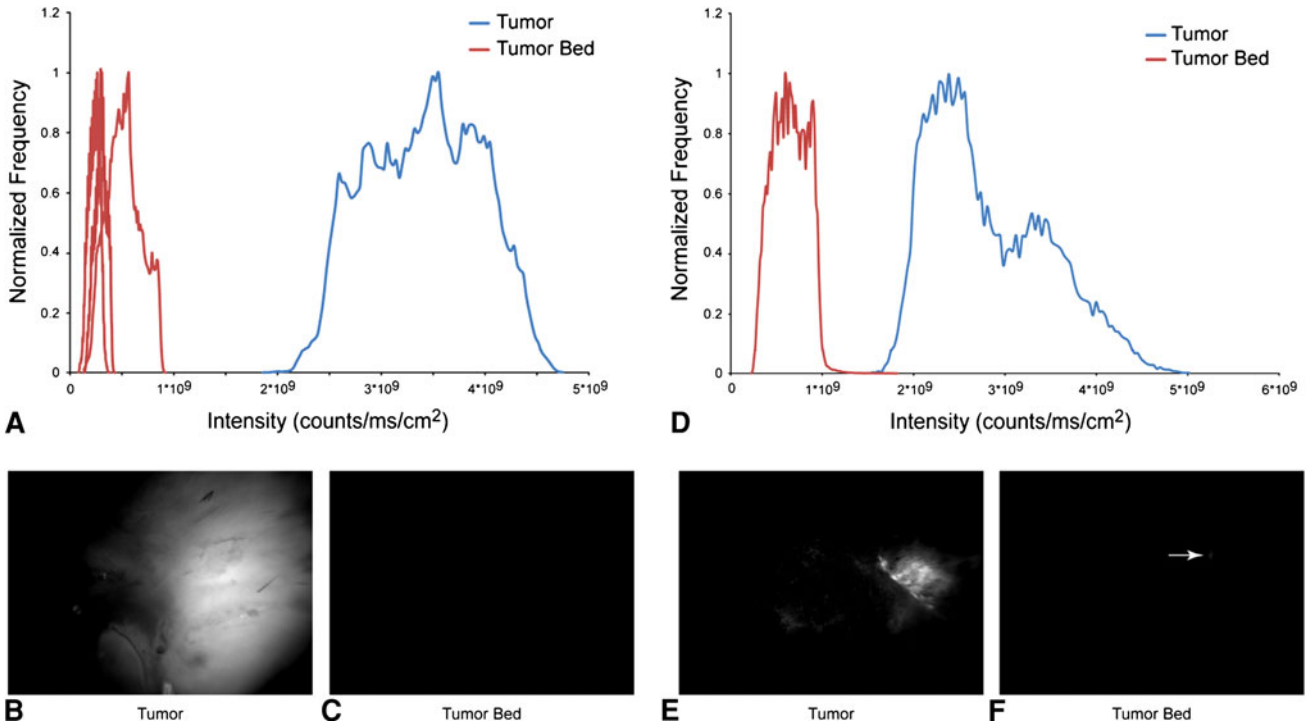

Fig. 2A–F Representative intraoperative imaging of the dogs is shown. Most of the dogs showed increased NIR fluorescence from tumor compared to images from the tumor bed. (**A**) An image-normalized intensity histogram shows distinct separation between (**B**) tumor and (**C**) tumor bed images. In contrast, in Dog 4 with an MCT, (**D**) an image-normalized intensity histogram shows a separation between (**E**) tumor and (**F**) tumor bed that is not as distinct; (**F**) a small area of residual fluorescence (arrow) was detected in the tumor bed after resection that was greater than the threshold of 80% of the minimum signal from the tumor.

CGTTGTGCTC-3′ and 5′-ACGCCGTGCTACTTCCTCA TTCTCT-3′; values were normalized to β2 M and RPS5 expression as described previously [4].

The closest surgical margin was determined by a single veterinary pathologist (SE) after gross examination of the specimen. The entire external surface of the specimen was then inked and the specimen was cut perpendicularly to the inked margin. Under microscopic examination, the distance between the tumor and the inked margin was measured, using sections selected by the pathologist. Frozen sections of both tumor and muscle (when available) within the tumor bed were evaluated. We used the analysis of frozen sections to guide microdissection of the tissues for isolation of RNA using the Ambion® RNAqueous® microkit (Life Technologies, Burlington, ON, Canada). Samples were included in this analysis if high-quality RNA tumor and normal muscle could be isolated (A260/280 $\geq$ 1.8). Because we were not able to isolate normal muscle from every dog and because in six samples (either tumor or matched normal muscle from the tumor bed) the RNA was not of sufficient quality, quantitative measurement of the expression of cathepsin proteases in tumors and matched normal muscle was performed in four dogs. Two of us (JKM, JEC) independently assessed all sections for cathepsin expression. For comparison, gene expression data from previously reported canine studies were downloaded from Gene Expression Omnibus [3, 11] and imported into GenePattern [16]. Data sets were combined using ComBat [7]. Multiple probes mapping to a single cathepsin were averaged together for the purposes of generating a heat map. Hierarchical clustering was performed using Pearson correlation row normalization.

Results

We identified no adverse reactions associated with administration of the probe. One dog developed a postoperative wound infection, which was successfully treated with débridement and antibiotics. In the six dogs where postoperative CBC and serum biochemistry profiles were available, there were no changes from baseline other than anemia consistent with operative blood loss in one dog.

The cathepsin-activated NIR probe was activated by all sarcomas. During imaging of the sectioned surface of resected tumors on the back table, fluorescence ranging from 3×10^7 to 1×10^9 counts/millisecond/cm^2 was apparent within all 10 tumors.

During intraoperative imaging of the tumor bed, no residual fluorescence above the threshold was detected

(Fig. 2A–C), except in one dog (Fig. 2D–F) (discussed below). In the rest of the dogs, quantitative analysis of fluorescence emission histograms showed no overlap between the emission rates for the primary tumor (Fig. 2B) and tumor bed (Fig. 2C). In the four dogs where quantitative assessment of the expression of cathepsin proteases was possible, expression of cathepsin proteases B (Fig. 3A), K (Fig. 3B), L (Fig. 3C), and S (Fig. 3D) was greater in tumor than in muscle from the tumor bed. Analysis of previously reported canine gene expression data [11, 19] showed overexpression of many cathepsin proteases in canine STSs compared to normal skeletal muscle (Fig. 3E).

Histopathologic assessment of surgical margins correlated with intraoperative imaging in nine of 10 tumors (Table 1). For eight tumors, intraoperative assessment of the tumor bed showed no residual fluorescence after resection, and correlative histopathologic examination of the resected tumors showed no extension of tumor to the inked margins. For one tumor, a Grade II MCT in Dog 4, intraoperative assessment of the tumor bed showed a focal area of residual fluorescence (Fig. 2D–F), and correlative histopathologic examination of the tumor showed a focal area of tumor extension to the inked margin. Adjuvant chemotherapy was given. Additional surgical resection was not performed. This dog has no evidence of recurrent disease at 10 months after surgery. Histopathologic assessment of surgical margins did not correlate with intraoperative imaging in one case. One dog with a Grade II malignant peripheral nerve sheath tumor (Dog 6) had no residual fluorescence within the tumor bed, but histopathologic assessment of the resected tumor showed a focal area of tumor extension to the inked margin. Post hoc review of the intraoperative images also revealed no residual fluorescence within the tumor bed. This dog did not receive additional resection or adjuvant therapy and has no evidence of recurrent disease at 11 months after surgery. At the time of this analysis, no dog in the study has developed recurrent disease.

Discussion

We developed an imaging system that can distinguish between normal tissue and cancer during oncologic resections. We previously demonstrated its efficacy in identifying and directing resection of microscopic residual sarcoma in a genetically engineered mouse model. To translate this technology toward clinical use, several critical questions that cannot be answered in a laboratory setting with a mouse model must be addressed. Therefore, we addressed the following questions: (1) Are any adverse clinical or laboratory effects observed after intravenous administration of the fluorescent probes to dogs undergoing resection of sarcomas? (2) Do naturally occurring canine sarcomas exhibit fluorescence after administration of the cathepsin-activated probes? (3) If so, is the tumor-to-background ratio sufficient to distinguish tumor from tumor bed during resection of naturally occurring canine tumors? And (4) can residual NIR fluorescence be detected in the tumor bed during surgery and does this correlate with a positive margin of the resected tumor?

Our study has some limitations. First, this clinical trial included a small number of dogs. Adverse effects of the probe or practical limitations of the imaging system may become apparent only after use in many individuals. Second, we had a relatively short followup to assess local recurrence. At the time of this analysis, no dog had recurrent disease. Given a local recurrence rate of 15% in dogs with STS [9], to evaluate the clinical performance of this imaging system with enough events related to recurrent disease, it will be necessary to include other veterinary hospitals to accrue sufficient dogs. Third, in one dog, we saw residual fluorescence, but we did not resect that area and therefore could not confirm by histology that the presence of residual fluorescence identified residual cancer within the tumor bed. Future studies will therefore utilize the imaging system to guide resection of the residual fluorescence so confirmatory histologic analyses can be performed. Fourth, the depth of visibility of fluorescent tissue with this system is not yet known. It is possible tumor cells deep to the exposed tumor bed are not detected because their fluorescence does not penetrate the normal tissue layer between the tumor cells and the imaging device.

We identified no obvious adverse clinical or laboratory effects from the NIR imaging probe VM249 when injected intravenously into the dogs at doses ranging from 0.5 to 2 mg/kg.

The cathepsin-activated NIR probe was activated by spontaneous naturally occurring canine sarcomas. In contrast to mice, the signal in the canine tumors exhibited a wider range of fluorescence emission (3×10^7 to 1×10^9 counts/millisecond/cm^2) consistent with a variety of disease sites and tumor types imaged. Just as we observed increased expression of cathepsin proteases in primary mouse sarcomas compared to normal muscle [12], we also observed increased expression of cathepsin proteases in naturally occurring canine sarcomas (Fig. 3). Interestingly, in tumor samples with available matched normal muscle and with RNA of sufficient quality for analysis, different sarcomas expressed different levels of cathepsin proteases. For example, the sarcoma in Dog 2 expressed relatively higher levels of cathepsins B and L, while the sarcoma in Dog 9 preferentially expressed cathepsins S and K. This suggests an NIR imaging probe such as VM249 that is activated by multiple cathepsin proteases may be most useful to image heterogeneous STSs. Nevertheless, our

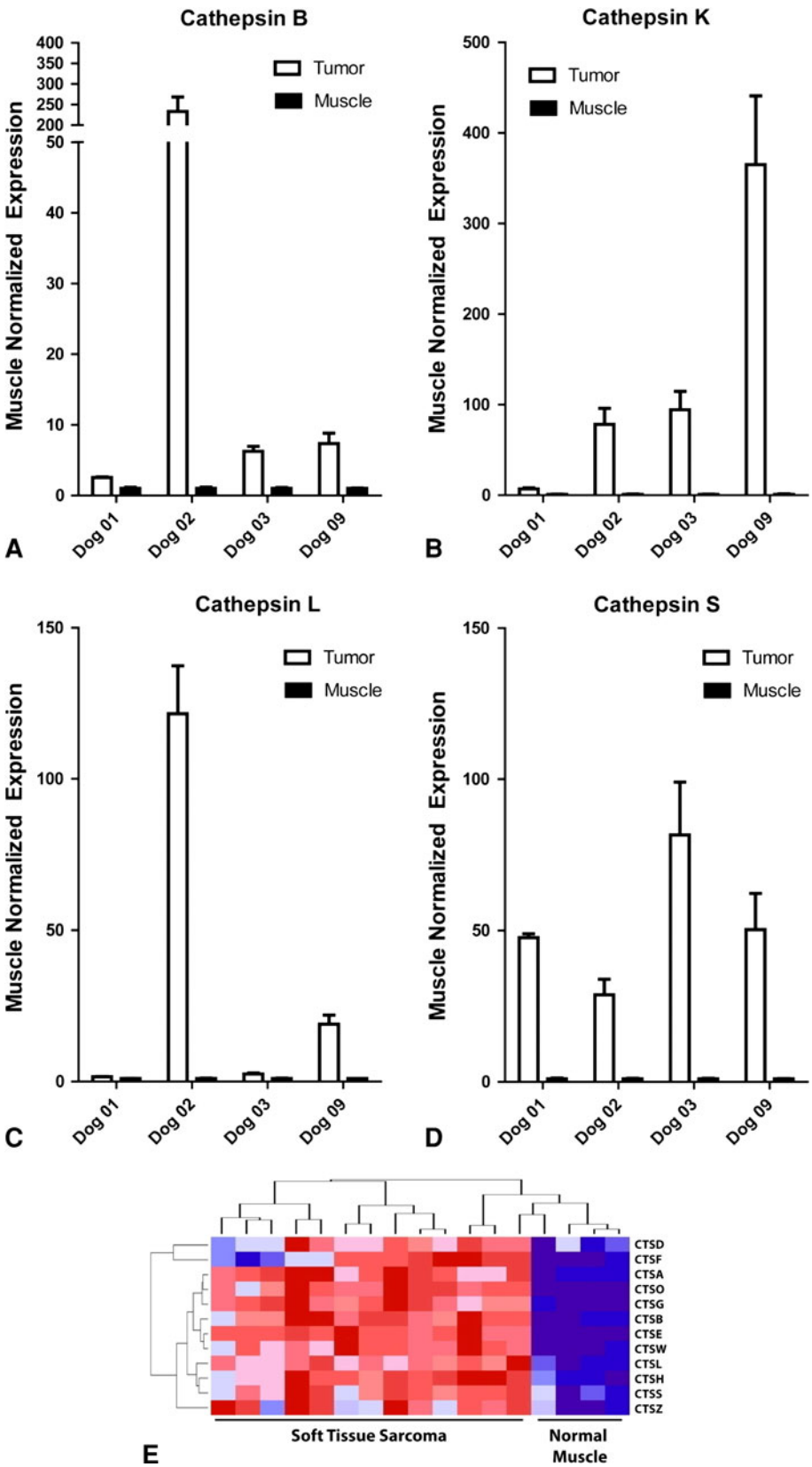

Fig. 3A–E Multiple cathepsin proteases that activate VM249 are upregulated in tumors compared to normal muscle as detected by quantitative real-time PCR: (**A**) cathepsin B, (**B**) cathepsin K, (**C**) cathepsin L, and (**D**) cathepsin S. (**E**) A heat map for a variety of cathepsins in canine STS and skeletal muscle is shown. Red indicates high levels of cathepsin expression whereas blue indicates low levels of cathepsin expression. CTSD = cathepsin D, CTSF = cathepsin F, etc.

observation that all tumors (n = 6 STSs and n = 4 MCTs) tested so far activated VM249 suggests most canine STSs express cathepsin proteases and indicates naturally occurring canine sarcomas exhibit fluorescence after administration of cathepsin-activated probes.

We found no residual fluorescence in nine tumor beds. Therefore, there is sufficient tumor-to-background signal ratio between sarcoma and adjacent normal tissue for this imaging system to distinguish tumor from tumor bed during surgery of naturally occurring canine sarcomas.

In one tumor bed (Dog 4), we detected a focus of residual NIR fluorescence above the threshold to score as positive residual fluorescence (Fig. 2, Table 1). This was one of two tumors the veterinary pathologist identified as having a positive margin. Therefore, in this tumor bed, positive residual fluorescence correlated with positive surgical margins on the excised tumor. In this dog, resection of this area of residual fluorescence might have been useful but was not permitted by our animal use protocol as this technology remained unproven in dogs, so modification of the surgeon's operative plan based on data from the device was prohibited. Future studies will allow such directed resection, which is, after all, the purpose of the technology. However, this dog was treated with systemic chemotherapy and remains disease free 10 months after surgery.

In Dog 6, a resected sarcoma was identified as having a focal positive margin, but in this case no residual NIR was observed in the tumor bed. It is possible, although the excised tumor had a focally positive margin, microscopic residual sarcoma was not present in the tumor bed. Consistent with this possibility, Dog 6 remains disease free 11 months after surgery even though this dog was not treated with adjuvant therapy. Alternatively, it is possible the positive surgical margin reflects a false-negative result of the imaging system, which could be due to a suboptimal dose of the probe, timing of probe administration relative to surgery, or detection threshold.

Our findings allow us to make several conclusions. Naturally occurring canine sarcomas express cathepsin proteases and activate the NIR imaging probe VM249. In addition, this imaging probe can be injected into dogs undergoing surgery without detectable adverse events. Moreover, the tumor-to-background signal ratio indicates this imaging system can discriminate tumor from adjacent normal tissue. Further clinical followup will be needed to correlate the imaging results with the development of recurrent disease. These initial results provide a proof of concept of this imaging system in an early phase trial in spontaneous sarcomas in dogs. Together with our data in primary sarcomas in mice [12], this study in dogs will serve as a precursor to clinical trials in humans with sarcoma.

Acknowledgments The authors thank our collaborators Moungi Bawendi, PhD, Linda Griffith, PhD, and W. David Lee, MS, at the Massachusetts Institute of Technology for valuable discussions regarding experimental design and data interpretation. We also thank Gary Spodnick, DVM, Brian Trumpatori, DVM, David Russlander, DVM, Angie Kozicki, DVM, and Stephen Engler, DVM, the collaborators from the multidisciplinary small animal oncology team at Veterinary Specialty Hospital of the Carolinas.

References

1. Allweis TM, Kaufman Z, Lelcuk S, Pappo I, Karni T, Schneebaum S, Spector R, Schindel A, Hershko D, Zilberman M, Sayfan J, Berlin Y, Hadary A, Olsha O, Paran H, Gutman M, Carmon M. A prospective, randomized, controlled, multicenter study of a real-time, intraoperative probe for positive margin detection in breast-conserving surgery. *Am J Surg.* 2008;196:483–489.
2. Barretina J, Taylor BS, Banerji S, Ramos AH, Lagos-Quintana M, Decarolis PL, Shah K, Socci ND, Weir BA, Ho A, Chiang DY, Reva B, Mermel CH, Getz G, Antipin Y, Beroukhim R, Major JE, Hatton C, Nicoletti R, Hanna M, Sharpe T, Fennell TJ, Cibulskis K, Onofrio RC, Saito T, Shukla N, Lau C, Nelander S, Silver SJ, Sougnez C, Viale A, Winckler W, Maki RG, Garraway LA, Lash A, Greulich H, Root DE, Sellers WR, Schwartz GK, Antonescu CR, Lander ES, Varmus HE, Ladanyi M, Sander C, Meyerson M, Singer S. Subtype-specific genomic alterations define new targets for soft-tissue sarcoma therapy. *Nat Genet.* 2010;42:715–721.
3. Briggs J, Paolini M, Chen QR, Wen X, Khan J, Khanna C. A compendium of canine normal tissue gene expression. *PLoS One*. 2011;6:e17107.
4. Brinkhof B, Spee B, Rothuizen J, Penning LC. Development and evaluation of canine reference genes for accurate quantification of gene expression. *Anal Biochem.* 2006;356:36–43.
5. Ehrhart N. Soft-tissue sarcomas in dogs: a review. *J Am Anim Hosp Assoc*. 2005;41:241–246.
6. Haid A, Knauer M, Dunzinger S, Jasarevic Z, Köberle-Wührer R, Schuster A, Toeppker M, Haid B, Wenzl E, Offner F. Intra-operative sonography: a valuable aid during breast-conserving surgery for occult breast cancer. *Ann Surg Oncol*. 2007;14:3090–3101.
7. Johnson WE, Li C, Rabinovic A. Adjusting batch effects in microarray expression data using empirical Bayes methods. *Biostatistics*. 2007;8:118–127.
8. Kirsch DG, Dinulescu DM, Miller JB, Grimm J, Santiago PM, Young NP, Nielsen GP, Quade BJ, Chaber CJ, Schultz CP, Takeuchi O, Bronson RT, Crowley D, Korsmeyer SJ, Yoon SS, Hornicek FJ, Weissleder R, Jacks T. A spatially and temporally restricted mouse model of soft tissue sarcoma. *Nat Med.* 2007;13:992–997.
9. Kuntz CA, Dernell WS, Powers BE, Devitt C, Straw RC, Withrow SJ. Prognostic factors for surgical treatment of soft-tissue sarcomas in dogs: 75 cases (1986–1996). *J Am Vet Med Assoc*. 1997;211:1147–1151.
10. Lewis JJ, Leung D, Casper ES, Woodruff J, Hajdu SI, Brennan MF. Multifactorial analysis of long-term follow-up (more than 5 years) of primary extremity sarcoma. *Arch Surg.* 1999;134:190–194.
11. Mahoney JA, Fisher JC, Snyder SA, Hauck ML. Feasibility of using gene expression analysis to study canine soft tissue sarcomas. *Mamm Genome*. 2010;21:577–582.
12. Mito JK, Ferrer JM, Brigman BE, Lee CL, Dodd RD, Eward WC, Marshall LF, Cuneo KC, Carter JE, Ramasunder S, Kim Y, Lee WD, Griffith LG, Bawendi MG, Kirsch DG. Intraoperative

detection and removal of microscopic residual sarcoma using wide-field imaging. *Cancer*. 2012. doi:10.1002/cncr.27458.
13. Mito JK, Riedel RF, Dodd L, Lahat G, Lazar AJ, Dodd RD, Stangenberg L, Eward WC, Hornicek FJ, Yoon SS, Brigman BE, Jacks T, Lev D, Mukherjee S, Kirsch DG. Cross species genomic analysis identifies a mouse model as undifferentiated pleomorphic sarcoma/malignant fibrous histiocytoma. *PLoS One*. 2009; 4:e8075.
14. Olson TP, Harter J, Munoz A, Mahvi DM, Breslin T. Frozen section analysis for intraoperative margin assessment during breast-conserving surgery results in low rates of re-excision and local recurrence. *Ann Surg Oncol*. 2007;14:2953–2960.
15. Pisters PW, Harrison LB, Leung DH, Woodruff JM, Casper ES, Brennan MF. Long-term results of a prospective randomized trial of adjuvant brachytherapy in soft tissue sarcoma. *J Clin Oncol*. 1996;14:859–868.
16. Reich M, Liefield T, Gould J, Lerner J, Tamavo P, Mesirov JP. GenePattern 2.0. *Nat Genet*. 2006;38:500–501.
17. Sabolch A, Feng M, Griffith K, Rzasa C, Gadzala L, Feng F, Biermann JS, Chugh R, Ray M, Ben-Josef E. Risk factors for local recurrence and metastasis in soft tissue sarcomas of the extremity. *Am J Clin Oncol*. 2012;35:151–157.
18. Sadoski C, Suit HD, Rosenberg A, Mankin H, Efird J. Preoperative radiation, surgical margins, and local control of extremity sarcomas of soft tissues. *J Surg Oncol*. 1993;52:223–230.
19. Welle MM, Bleyt CR, Howard J, Rufenacht S. Canine mast cell tumours: a review of the pathogenesis, clinical features, pathology, and treatment. *Vet Dermatol*. 2008;19:321–339.